Special Section: Frontiers of Hydropedology in Vadose Zone Research

Hu Zhou
Xinhua Peng*
Frédéric Darboux

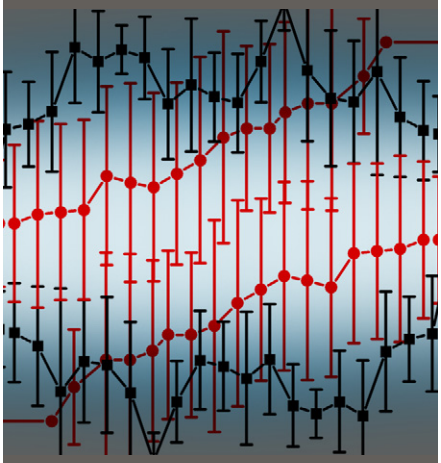

A laboratory rainfall simulation showed that Ultisols are prone to crusting and rainfall kinetic energy is a major driver of crust formation. This crusting reduced infiltration significantly and so promoted water and particle runoff. Mulching could be an effective way to alleviate crusting, to conserve more water, and to reduce erosion.

H. Zhou and X. Peng, State Key Lab. of Soil and Sustainable Agriculture, Institute of Soil Sciences, Chinese Academy of Sciences, 71 East Beijing Rd., Nanjing 210008, P.R. China; F. Darboux, INRA, UR0272, UR Science du sol, Centre de recherché Val de Loire, CS 40001, F-45075 Orléans Cedex 2, France. *Corresponding author (xhpeng@issas.ac.cn).

Vadose Zone J.
doi:10.2136/vzj2013.01.0010
Received 14 Jan. 2013.

Effect of Rainfall Kinetic Energy on Crust Formation and Interrill Erosion of an Ultisol in Subtropical China

Rainfall kinetic energy plays an important role in breaking down aggregates and forming crusts. A laboratory rainfall simulation study was conducted on an Ultisol from subtropical China to investigate the effect of rainfall kinetic energy on crusting, infiltration, runoff, and erosion. Two treatments, that is, high kinetic energy (HKE) and low kinetic energy (LKE), were applied during this study. Air-dried soil was packed in a soil box (50 by 50 cm), and the soil box was subjected to 38 mm h^{-1} rainfall with three replicates. The runoff, splash, erosion, and percolation were measured during the simulation. For each treatment, an additional soil box was dedicated to sampling the undisturbed soil samples at different time intervals to make thin sections. The entire soil surface was covered by structural or sedimentary crust at the end of the experiment. When compared with the HKE rainfall, the LKE rainfall reduced the direct physical impact of raindrops that disintegrated the soil aggregates and compacted the soil surface; therefore, the LKE preserved the soil infiltration capability and subsequently postulated the formation of crust. This resulted in a higher infiltration rate and greater cumulative infiltration and percolation but lower splash, runoff, and soil erosion in the LKE treatment compared with the HKE treatment. The results show that Ultisols are prone to crusting and that rainfall kinetic energy is a major driver of crust formation. This finding indicates that mulching the soil surface is an effective way to alleviate crusting, to conserve more water, and to reduce erosion.

Abbreviations: HKE, high kinetic energy; KE, kinetic energy; LKE, low kinetic energy.

Crusting is very common in soils exposed to rainfall. The physical crusts can severely affect the soil hydrological processes (e.g., decreasing infiltration, increasing runoff) and can lead to soil erosion (Le Bissonnais and Singer, 1992; McIntyre, 1958a; Moore and Singer, 1990). In addition, the crust can impede seeding emergence (Awadhwal and Thierstein, 1985). To better manage the crust-prone soil and to accurately predict the hydrological processes, it is necessary to understand the mechanism of crust formation and its effects on related hydraulic characteristics.

Crust formation has been extensively studied. The common processes include the breakdown of aggregates, particle displacement and rearrangement, and surface compaction (Le Bissonnais, 1990; Le Bissonnais et al., 1989; McIntyre, 1958a; Norton, 1987; Slattery and Bryan, 1994). Raindrop impact is a major driver of aggregate breakdown and surface compaction (Betzalel et al., 1995; Mcintyre, 1958b; Morin et al., 1981; Morin and Van Winkel, 1996; Shainberg and Singer, 1988; Smith et al., 1990). Rainfall with high kinetic energy increases soil detachment and compaction, prompting the formation of soil crust (Shainberg and Singer, 1988; Smith et al., 1990). Lowering the rainfall kinetic energy, on the other hand, results in decreased mechanical breakdown of soil aggregates and soil splash (Levin et al., 1991), which helps conserve the structure of surface soil aggregates; therefore, soil crust formation is delayed or eliminated. Earlier studies (Morin and Van Winkel, 1996; Shainberg and Singer, 1988) found that crusts formed slower under LKE rainfall, but crusts could still form under very LKE rainfall.

Crust formation can sharply decrease the infiltration rate and increase water runoff and erosion (e.g., Levin et al., 1991; Morin et al., 1981; Morin and Van Winkel, 1996). Levin et al. (1991) found that an increase in the rainfall kinetic energy reduced the final infiltration rate and cumulative infiltration and increased erosion of smectite-dominant soils. Reichert et al. (1994) noted that rain kinetic energy influenced the erosion rates

less as the soil sealed and consolidated. The interaction among rainfall kinetic energy, crust formation, and runoff and erosion can be manifested by the dynamics of soil surface structure during rainfall. Changes in the soil pore structure, resulting from disintegration or translocation of soil aggregates, determines the proportioning of rainfall into runoff or infiltration (Arshad, and Mermut, 1988; Miralles-Mellado et al., 2011). The microstructure of soil crust has been studied by thin section (two-dimensional) or computed tomography (three-dimensional) and quantified with digital image analysis (Lee et al., 2008). However, the dynamics of pore structure during crusting are seldom studied.

Most of the studies on crusting were conducted on unstable loam soils in arid-to-temperate climates (e.g., Moore and Singer, 1990; Le Bissonnais and Singer, 1992). Clayey soil in the tropical and subtropical areas received less attention. The Ultisols (red clay soil), rich in clay and low in exchangeable Na, are mostly distributed in humid temperate or tropical regions. In China, they are located in the hilly areas of the tropical or subtropical South and cover an area of 1.14 million km^2 (Shi et al., 2010; Yang et al., 2012). Ultisols are prone to erosion, partially because of the hilly topography and the heavy rainstorms during the summer because of the monsoon regime. A recent survey found that more than 15% of the land in this region is submitted to erosion (Liang et al., 2008). Both rainfall simulation experiments (Hu et al., 2005; Li et al., 2005) and field observations found that crusts formed after storms. However, little is known about the mechanism of crust formation and the effect of crusts on water and particle transfers in Ultisols. The objectives of this study were as follows: (i) to examine the crusting mechanisms of the Ultisol and (ii) to evaluate the effect of rainfall kinetic energy on the crusting process and soil splash, runoff, and erosion. The consequences of the findings for agricultural management are also discussed.

Materials and Methods

Soil Sample

The surface layer (0–15 cm) of an Ultisol was collected from cultivated peanut fields at the Red Soil Ecological Experiment Station (Chinese Academy of Sciences) located in Yingtan, Jiangxi Province, China (116°5′30″E, 28°5′30″N). This region has a typical subtropical warm humid climate. The long-term (2000–2010) mean annual precipitation is 1706 mm, with more than 60% of it falling from March to July. The soil is developed from kaolinitic Quaternary red clay and has a clay texture (Table 1). The collected soil was air-dried and sterilized using Gamma-ray before being shipped to France. To improve the repeatability, the soil samples used to fill the soil trays were first hand-sieved into different aggregate size classes (the percentage of aggregates larger than 5 mm was less than 5%) and were then mixed using a prescribed weight size distribution (3–5 mm, 17.5%; 2–3 mm, 16.3%; 1–2 mm, 17.5%; 0.5–1 mm, 23.7%; < 0.5 mm, 25%).

Table 1. Selected physical and chemical properties of the Ultisol.

Property†	Value
Sand ($g\,kg^{-1}$)	232
Silt ($g\,kg^{-1}$)	356
Clay ($g\,kg^{-1}$)	411
SOM ($g\,kg^{-1}$)	11.5
pH (1:2.5 H_2O)	5.0
Fe_t ($g\,kg^{-1}$)	36.3
Fe_{DCB} ($g\,kg^{-1}$)	33.1
CEC ($cmol\,kg^{-1}$)	10.5
Exchangeable Na ($cmol\,kg^{-1}$)	0.19

† SOM, soil organic matter; Fet, total Fe; Fe_{DCB}, extractable Fe with dithionite-citrate-bicarbonate solution; CEC, cation exchange capacity.

Soil Box Preparation

The soil trays employed in this rainfall simulation study were designed to simultaneously measure runoff, splash, and percolation as shown in Fig. 1 (Fox et al., 1998; Leguédois and Le Bissonnais, 2004). The experimental surface area of the soil trays was 50 by 50 cm (10 cm in depth) surrounded by a 10-cm buffer to compensate for splash. The soil trays were set to a 5% slope. On the downslope side of the test area, the box included a runoff collector with an outlet at the bottom. The base of the test area was made of a perforated board overlaid with a piece of geo-textile to permit drainage of the infiltration water. An outlet at the bottom allowed for the collection of percolated water (Fig. 1). The soil was carefully packed with successive 2-cm layers to avoid aggregate segregation and to ensure a constant bulk density of 1.2 $Mg\,m^{-3}$. The upslope buffer zone was kept empty to allow for the installation of the splash collector (Leguédois and Le Bissonnais, 2004). Within the experimental area, the soil surface was shaped into a ridge-and-furrow morphology to replicate field roughness. Five ridges and four furrows, oriented parallel to the slope, were made for each replicate (Fig. 1). The height difference between ridges and furrows was approximately 1 cm.

Rainfall Simulation Experiment

The rainfall simulator, similar to the one described in Foster et al. (1979), was equipped with oscillating nozzles and was located 6 m above the soil surface. It produces rainfall with a drop velocity-drop size relationship similar to natural rainfall. Rainfall intensity was controlled by the nozzle type (Spraying Systems Co., Illinois, USA. Veejet 65150), the water pressure (1 bar), and the sweep frequency (27.5 sweeps/min). It was set to produce a rainfall intensity of 38 $mm\,h^{-1}$ during over the course of 1.5 h. Deionized water was used throughout the whole experiment.

Two treatments, that is, HKE rainfall and LKE rainfall, were used. For the HKE treatment, soil trays were subjected to rainfall that fell directly from the simulator. For the LKE treatment, a screen

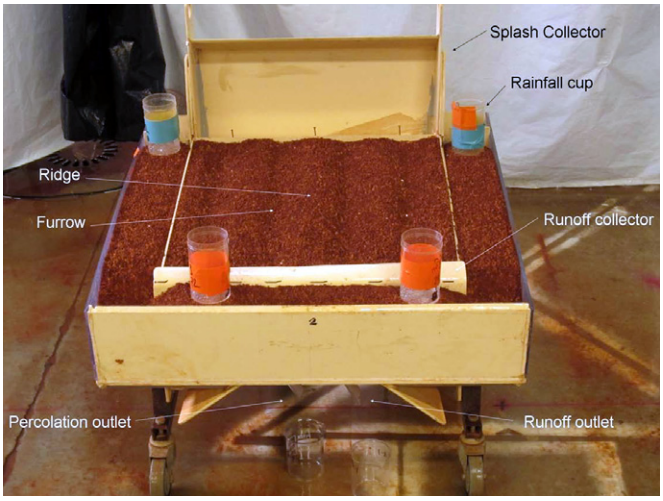

Fig. 1. Design of the experimental soil box and soil surface preparation.

with a mesh size of 2 mm was set 50 cm above the soil surface to intercept the rainfall, thereby reducing the rainfall kinetic energy. A laser raindrop spectrometer (Thies Laser Distrometer, Thies Clima, Germany) was used to measure the size and velocity distributions of the raindrops. From these data, the rainfall kinetic energy was calculated. The kinetic energy for the HKE and LKE treatments was 9.3 and 4.6 J m^{-2} mm^{-1}, respectively.

For each treatment, three replicates were conducted for the collection of runoff, splash, and percolation. Samples of runoff and percolation were collected into beakers at the downstream side of the soil trays every 1 or 2 min (depending on the flux). Runoff samples were weighed before and after oven drying (105°C) to calculate the water runoff and soil erosion. Splash samples were collected using a splash collector located at the upstream side of the soil tray every 9 min. The splash samples were oven-dried at 40°C, and their aggregate size distribution was determined by hand sieving. Infiltration rates were calculated by the difference between the rainfall intensity and the water runoff rate.

An additional replicate for each treatment was conducted to collect samples for studying the soil surface morphology and micromorphology. During the rainfall, parts of the ridges and furrows were covered with lids (10 by 8 cm) at 0, 10, 20, 40, 60, and 90 min (corresponding to 6, 12, 25, 38, and 57 mm of rainfall, respectively) to preserve the structure of the underlying soil. To avoid changes by incoming overland flow, the upstream flow was blocked by a plastic plate inserted vertically upstream from the lid and diverted to the box outlet. A total of 20 undisturbed samples were taken several days later with aluminum Kubiena boxes (7 by 5.5 by 5 cm), when the soil was not too sticky. Photos of the sample surfaces were taken, and then the samples were air-dried at room temperature for soil thin section preparation.

Soil Thin Section Preparation and Analysis

The air-dried undisturbed samples were oven dried at 40°C for 24 h and then impregnated under vacuum (8 h) with polyester resin mixed with 30% of styrene monomer. After 2 mo of hardening at room temperature, the vertically oriented thin sections (30 μm in thickness, 5 by 3.5 cm in size) were made according to the procedure described by Murphy (1986). Soil thin sections were examined using an Olympus polarized microscope, and the micromorphological characteristics were described following Stoops (2003). Photos were taken using a camera equipped on the microscope both under plain light and polarized light. The size of the photos was 2560 by 1920 pixels with a pixel size of 0.12 by 0.12 μm. Photos of the thin sections were converted to grayscale images and then to binary images with threshold values based on visual observation. The pores were identified by subtraction of cross-polarized images from the corresponding plain polarized images. Porosity was measured with Matlab (The MathWorks Inc., Natick, MA).

Statistical Analysis

To compare differences in runoff, percolation, splash, and erosion caused by runoff between the two treatments, a t test was conducted using SAS software (SAS institute, 1990) at the $p = 0.05$ level. The porosities of the surface soil were measured without replicate; therefore, no statistical analysis was conducted. This analysis was done only to show the trend.

Results

Soil Surface

Because the soil surface was shaped into a ridge-and-furrow morphology, the surface of the ridges and of the furrows showed contrasting histories. On the ridges of the HKE treatment, after 6 mm of rainfall, the aggregates located directly at the surface were partly broken down, leading to a relative smoothening of the surface (Fig. 2a). However, numerous aggregates still appeared as isolated fragments with distinguishable shapes. At the next step (12 mm of rainfall), more aggregates had disaggregated and the size of the remaining distinguishable aggregates had decreased. At 25 mm of rainfall, few isolated aggregates could still be observed. At this step, overland flow had started, washing away most of the small-sized aggregates. The soil surface became smoother and sealed. In the last two steps (38 and 57 mm of rainfall), the surface became even smoother and only very few aggregates could be observed with the naked eye. The soil surface that was subjected to LKE rainfall showed an evolution similar to the HKE treatment but at a slower pace (Fig. 2b). Many well-formed isolated aggregates were observed even after 25 mm of rainfall. At 38 mm, fewer aggregates were present at the ridge surface. At 57 mm, aggregates were still present, but the surface had sealed.

The soil surface within the furrows behaved similarly at the beginning to that on the ridges. However, after the runoff started (between the 12 mm and 25 mm of rainfall for HKE and between

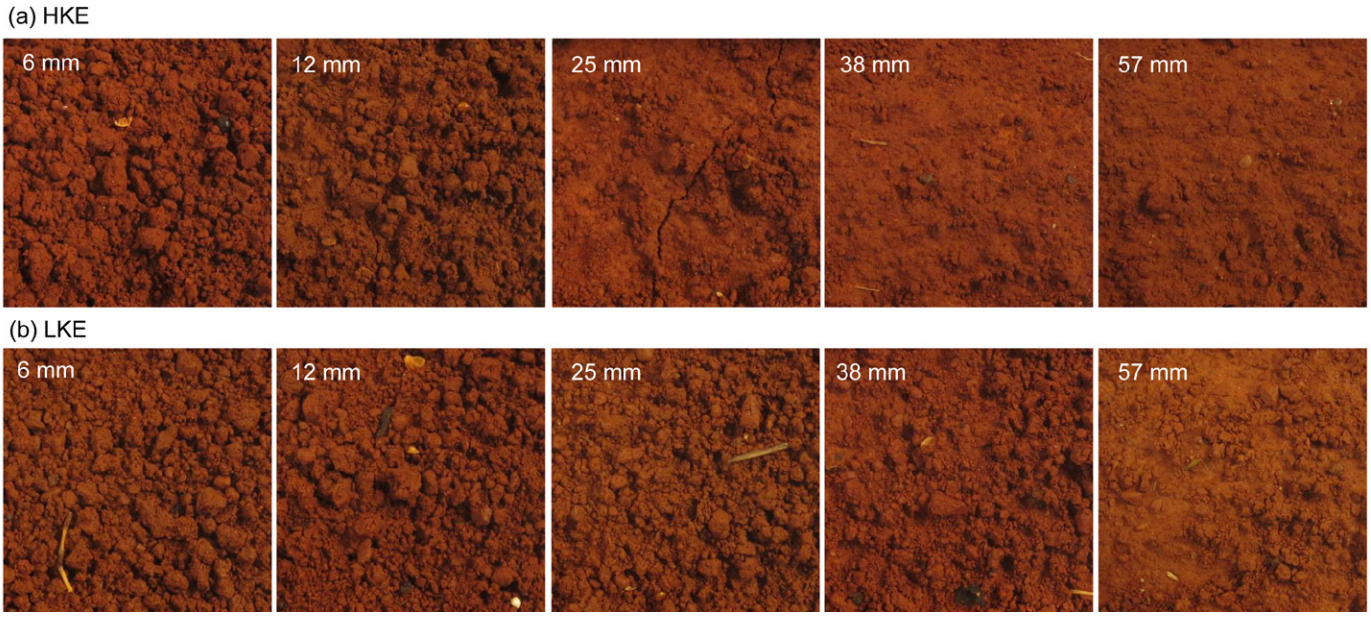

Fig. 2. Evolution of the soil surface at the ridges with cumulative rainfall during the simulation for the (a) high kinetic energy and (b) low kinetic energy treatments. Frame size: 4.2 by 4.2 cm.

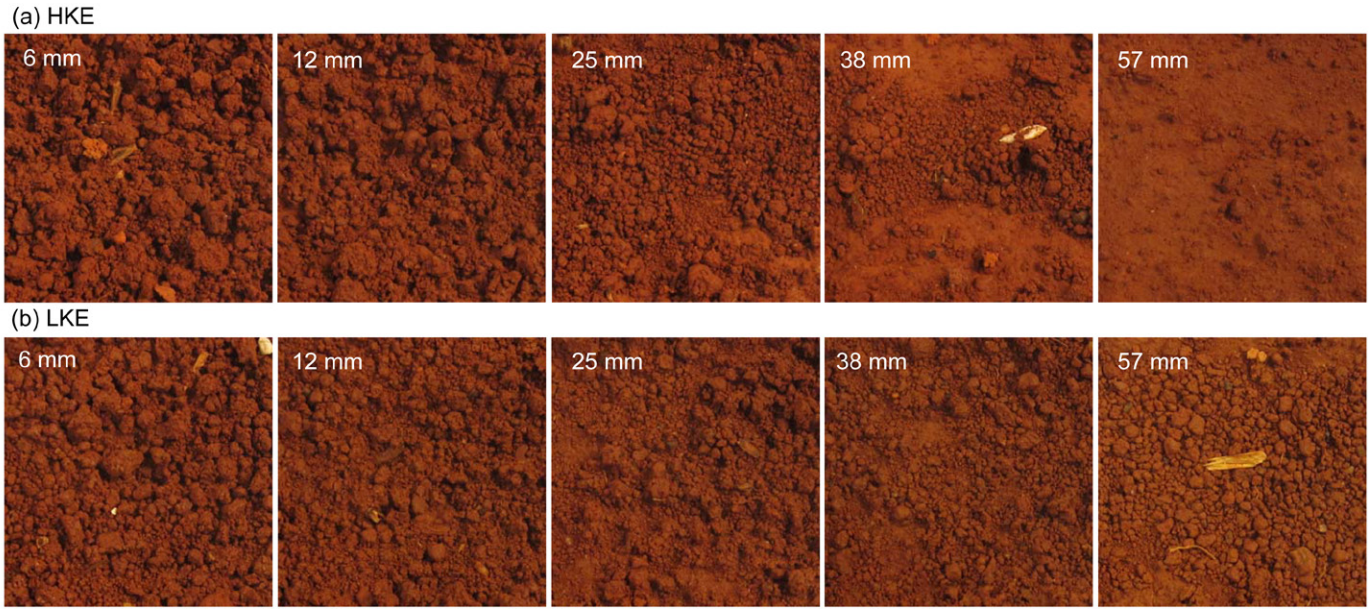

Fig. 3. Evolution of the soil surface at the furrows with cumulative rainfall during the simulation for the (a) high kinetic energy and (b) low kinetic energy treatments. Frame size: 4.2 by 4.2 cm

the 25 mm and 38 mm of rainfall for LKE), the breakdown products of aggregates from the ridges were washed down or splashed into the furrows (Fig. 3a). For the HKE treatment, many aggregates were observed at 38 mm of rainfall, but at the 57 mm of rainfall, they were much less numerous and the surface looked smooth and sealed. For the LKE treatment, on the other hand, numerous aggregates were still present on the furrow surface at 57 mm of rainfall (Fig. 3b).

Crust Micromorphology

The micromorphological observation of vertical thin sections helps identify soil crust development. Two types of crusts were observed in this study: structural crusts on the ridges and sedimentary

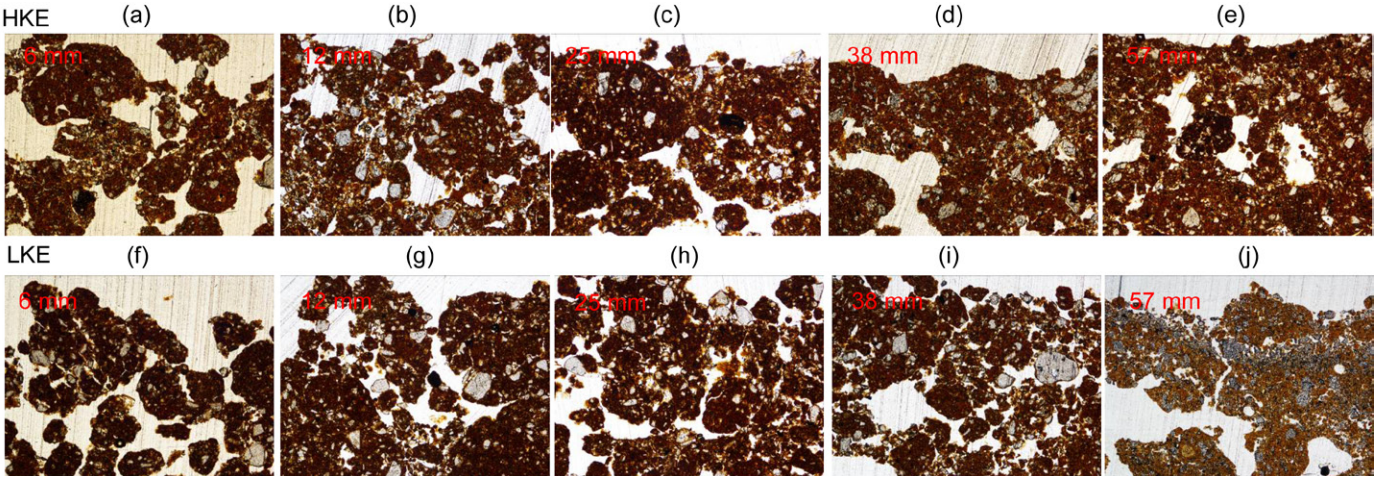

Fig. 4. Evolution of structural crust on the ridges with cumulative rainfall during the simulation for the (a–e) high kinetic energy and (f–j) low kinetic energy treatments. Frame size: 3.1 by 2.3 mm

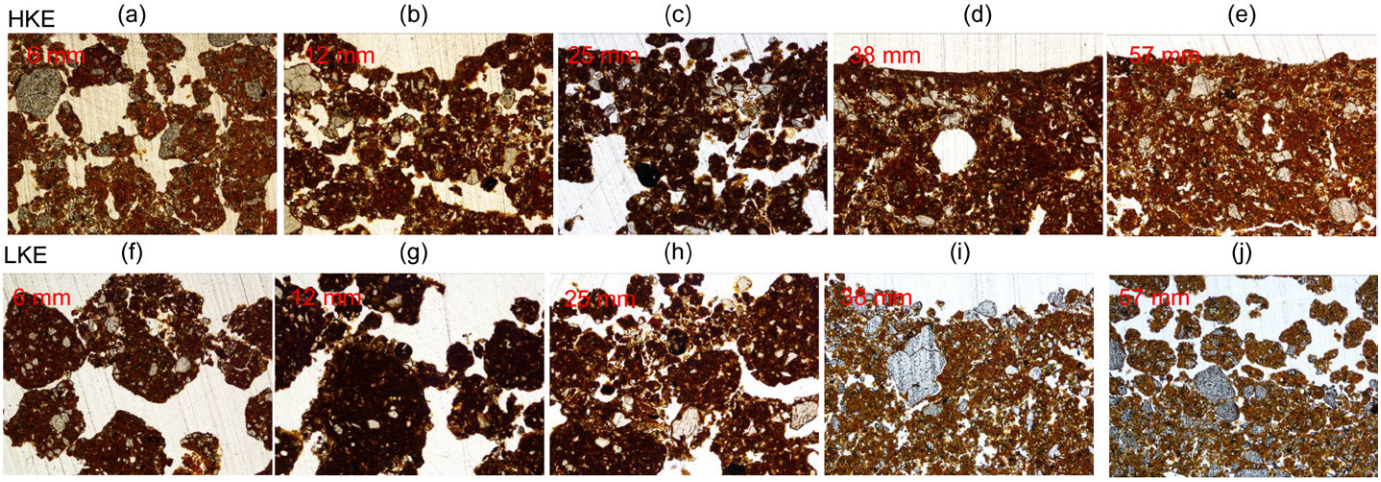

Fig. 5. Evolution of sedimentary crust in the furrows with cumulative rainfall during the simulation for the high kinetic energy and low kinetic energy treatments. Frame size: 3.1 by 2.3 mm

crusts in the furrows (Fig. 4 and 5). The soil structure immediately under the surface was not affected by rainfall in either the HKE or LKE treatments. This result shows that crusting occurred (and not hard-setting).

On the ridges, after receiving 6 mm of rain, the isolated macroaggregates were visible and the inter-aggregate pores were inter-connected and continuous to the surface for both the HKE and LKE treatments (Fig. 4a and 4f). Microcracking, known to be caused by differential swelling (Le Bissonnais, 1996), was observed in some aggregates at the uppermost layer (Fig. 4a and 4f). With the continuing application of HKE rainfall, the aggregates at the surfaces broke down, most likely due to slaking and mechanical raindrop impact. The pores that opened to the surface got clogged with fine fragments (Fig. 4b and 4c) and the porosity decreased (Fig.6a). A thin crust (0.3–0.8 mm) was formed at 38 mm of HKE rainfall (Fig. 4d and 4e) and persisted, as indicated by the stable porosity (Fig. 6). For the LKE rainfall, it took more time for the aggregates to break down (Fig. 4j and 4i), and a structural crust was clearly formed only at the end of the experiment. The porosity of surface soil in the LKE treatment was higher than the HKE treatments for the same cumulative rainfall (Fig. 6).

The dynamics of surface structure in the furrows were similar to those on the ridges until runoff began (Fig. 5c–5e and 5i–5j). Then, a sedimentary crust started to form, with a thickness that was usually >1 mm. The sedimentary crust incorporated aggregates larger than those of the structural crusts. Overland flow most likely

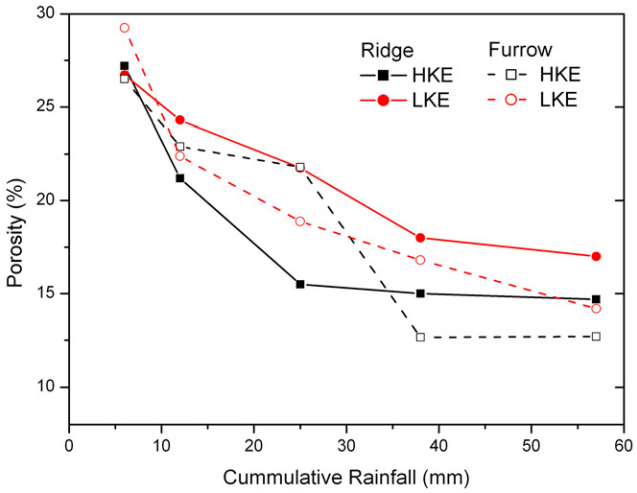

Fig. 6. Change in porosity of the surface soil of ridges and furrows with cumulative rainfall for the high kinetic energy and low kinetic energy treatments.

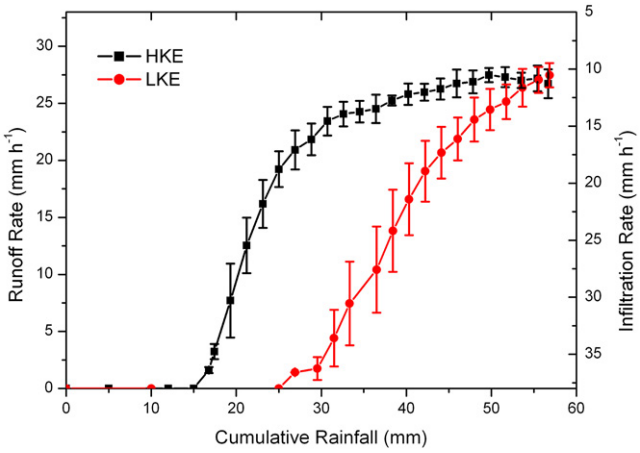

Fig. 7. Change of runoff and infiltration with cumulative rainfall for the high kinetic energy and low kinetic energy treatments.

brought these aggregates from the ridges to the furrows. Part of them contributed to runoff, while others were deposited in the furrows. Compared to the smooth surface of the sedimentary crust in the HKE treatment, many macroaggregates were still observed in the LKE treatment. Those aggregates, which slid from the ridges, stayed on the surface for a longer duration before adding to runoff, most likely because the surface water protected them from raindrop impact. By comparing Fig. 5i and 5j, it can be noted that such macroaggregates were deposited on top of the sedimentary crust. This finding is consistent with the numerous aggregates observed on the furrow surface for the LKE treatment at 57 mm of rainfall (Fig. 3b), as mentioned in the previous section. Changes in the porosity of the surface soil showed a similar trend as on the ridges, except that the final porosity was lower for the furrows (Fig. 6). This result can be explained by the deposition of particles that clogged the inter-aggregate pores.

Runoff, Infiltration, and Percolation

The runoff and infiltration rates as a function of cumulative rainfall are presented in Fig. 7, and their cumulative amounts are listed in Table 2. For the HKE treatments, the runoff started after the soil received 14 mm of rainfall. The runoff rate increased sharply at first and then increased slowly up to a near steady state rate of ~27 mm h^{-1} after 50 mm of rainfall. Runoff of the LKE treatment started after 28 mm of rainfall and then increased progressively to a final rate similar to that of the HKE treatment at the end of the experiment. These final runoff rates are equivalent to a runoff coefficient of 71%.

The infiltration rate showed an inverse trend to the runoff rate (Fig. 7). The infiltration rate of soils receiving HKE rainfall dropped rapidly with the cumulative rainfall until the soil crusts were roughly formed (25 mm of rainfall, Fig. 4 and 5) and then gradually declined to a near steady–state rate of 11 mm h^{-1} when

Table 2. Cumulative water runoff, infiltration, splash, percolation, and soil erosion for the HKE and LKE treatments during the simulation.

Cumulative amount	HKE	LKE
Water runoff (mm)	23.3 (1.0) †a‡	16.9 (2.9)b
Infiltration (mm)	33.7 (1.0)b	40.1 (2.9)a
Percolation (mm)	0.0 (0.0)b	5.8 (0.6)a
Splash (g)	45.8 (0.6)a	3.7 (0.1)b
Soil erosion (g m^{-2})	87.7 (8.5)a	22.9 (13.1)b

† Values in parentheses represent the standard deviation of the mean.
‡ Values in the same rows followed by different letters are significantly different ($p < 0.05$).

the crust was well formed (Fig. 4 and 5). The infiltration rate of soil receiving LKE rainfall, on the other hand, decreased almost linearly with the cumulative rainfall up to a final rate of 11 mm h^{-1}. The total infiltration, which was calculated by integrating the infiltration rate over time, was significantly higher ($p < 0.05$) in the LKE treatment than in the HKE treatment (Table 2).

Pronounced differences in percolation were found between the HKE and LKE treatments (Fig. 8). No percolation was observed for the HKE treatment throughout the whole experiment, whereas for the LKE treatment, the percolation started after 36 mm of rainfall. The percolation rate increased to 14 mm h^{-1} after 46 mm of rainfall and then decreased to 9.5 mm h^{-1} at the end of the experiment.

Splash and Erosion Caused by Runoff

The amount of splash from the soil receiving the LKE rainfall was significantly lower ($p < 0.05$) than that from the soil receiving the HKE rainfall (Fig. 9). The splash from the soil receiving the HKE rainfall increased to 0.78 g min^{-1} after receiving 27 mm rainfall and afterward decreased to a final rate of 0.60 g min^{-1}. The

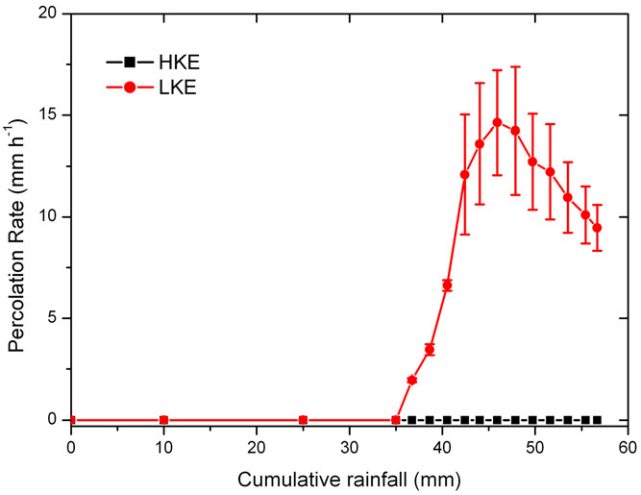

Fig. 8. Change of percolation with cumulative rainfall for the high kinetic energy and low kinetic energy treatments.

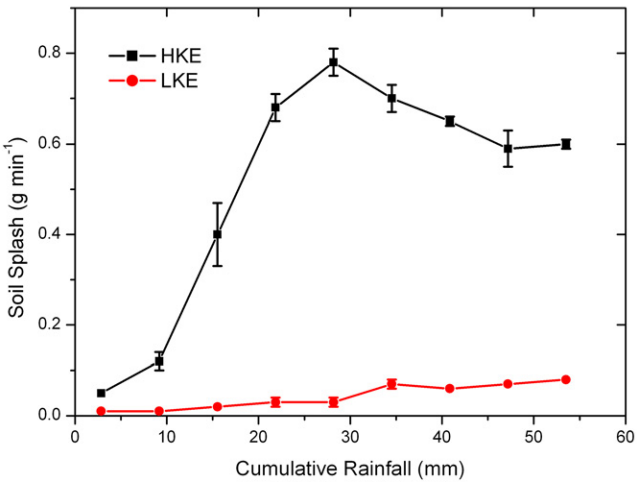

Fig. 9. Change of splash with cumulative rainfall for the high kinetic energy and low kinetic energy treatments.

splash from the soil receiving the LKE rainfall was much lower and reached a maximum rate of 0.08 g min^{-1} at the end of the rainfall.

The soil erosion caused by runoff started with water runoff initiation. The erosion followed a pattern similar to that of the water runoff (Fig. 10). Erosion from the HKE treatment increased with increasing runoff rate, reaching a near steady state (~1.5 g m^{-2} min^{-1}). After the crusts were well formed (at approximately 30 mm of rainfall), the erosion rate tended to decrease. Erosion from the LKE treatment increased continuously with the cumulative rainfall but at a lower speed (Fig. 10). During the simulation, the erosion from the LKE treatment was always lower than that from the HKE treatment.

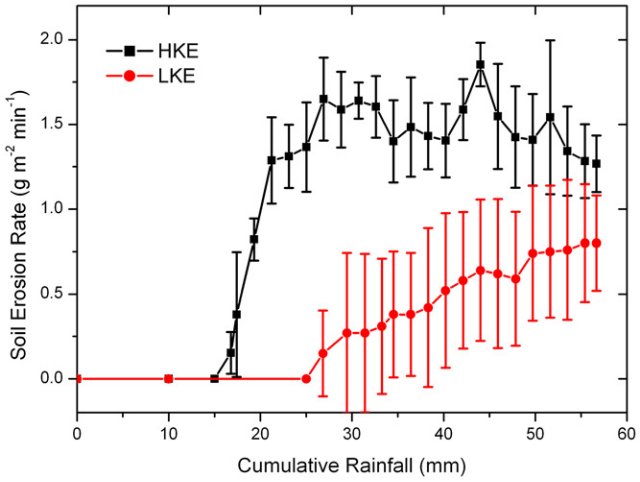

Fig. 10. Change of soil erosion rate with cumulative rainfall for the high kinetic energy and low kinetic energy treatments.

Discussion

Crust Formation Processes

The aggregates of Ultisols that developed from kaolinitic Quaternary red clay are stable because of their high kaolinitic-clay content and are therefore believed to be unsusceptible to crusting (Li et al., 2005). However, the rainfall simulation experiment showed the development of crusts. In this study, the ridge-and-furrow morphology of the soil surface favored the formation of both structural and sedimentary crusts simultaneously. Evolution of the soil surface was similar at the beginning on the ridges and furrows. Differences were observed after runoff began. Based on micromorphological observation and quantification of the porosity of the surface soil, the evolution of the crusts can be divided into four stages: (i) initial wetting of the soil, with some cracks formed in the aggregates at the surface; (ii) surface aggregate breakdown; (iii) aggregate displacement and rearrangement by raindrop impact, as shown by the initiation of splash. With the continuous increase of cumulative rainfall, surface ponding occurred, leading to runoff. The breakdown products of aggregates on the ridges were carried down to the furrows by overland flow or splash. Some of the displaced aggregates reached the outlet, while others were deposited at the soil surface or clogged the inter-aggregate pores, decreasing the infiltration rate. (iv) Finally, surface compaction by raindrop impact (for the structural crust) or by sedimentation (for the sedimentary crust). During this process, soil surface roughness decreased gradually and finally became very smooth when the crust was well formed, especially for the HKE treatment. The crusting stages are consistent with previous studies (Le Bissonnais, 1990; Le Bissonnais et al., 1989; McIntyre, 1958a; Norton, 1987; Slattery and Bryan, 1994).

Soils receiving HKE and LKE rainfalls showed similar crusting stages. However, it took a much longer time for the aggregates of the LKE treatment to break down and thereafter to form a crust.

This result can be explained by the effect of rainfall kinetic energy in breaking down aggregates. Indeed, raindrops play an important role in aggregate disintegration by direct mechanical impact (Betzalel et al., 1995; Mcintyre, 1958b; Morin et al., 1981; Morin and Van Winkel, 1996; Shainberg and Singer, 1988; Smith et al., 1990). In fact, the main mechanisms of aggregate breakdown are slaking, microcracking, and mechanical breakdown (Le Bissonnais et al., 1989; Le Bissonnais, 1996). Slaking and microcracking can only occur during soil wetting. Because the wetting rates at the surface were identical (i.e., same rainfall intensity), these two mechanisms are unlikely to be responsible for the difference in crust development. On the contrary, mechanical breakdown, related to raindrop impact, can continue during the entire rainfall (Legout et al., 2005). Hence, the observed crust formation is likely to be mostly related to the effect of rainfall kinetic energy on aggregates breaking down. The mechanical impact was lower in the LKE treatment than in the HKE treatment. The lower raindrop kinetic energy explains both the slower aggregate disaggregation and the lower splash rate (Levin et al., 1991). Moreover, the lower raindrop kinetic energy may have also reduced the soil surface compaction by raindrop impact (Shainberg and Singer, 1988).

Crusting, Infiltration, Percolation, Splash, and Erosion

The dynamics of water runoff were controlled by the temporal change of the infiltration rate, which was closely related to the dynamics of the pore structure during the crusting process. During rainfall, the infiltration rate decreased with time and finally reached a nearly constant value for the HKE treatment (Fig. 7). Both crusting (decrease of porosity) and the decrease of the hydraulic gradient could cause a decrease in the infiltration rate during rain (Le Bissonnais and Singer, 1992). Despite the fact that the hydraulic gradient was not measured in this study, the effect of crusting on infiltration could be shown by comparing the dynamics of the infiltration rate between the HKE and the LKE treatments. First, runoff started earlier for the HKE treatment compared with the LKE treatment. Because the rainfall started with the same initial soil condition for both treatments, the only reason for the difference in infiltration rate may come from the difference in rainfall kinetic energy. For the HKE treatment, the aggregates were broken down quicker and clogged the pores faster (Fig. 6), reducing the infiltration rate more rapidly. Second, the HKE treatment had less cumulative infiltration compared with the LKE treatment during the experiment, which would result in a higher hydraulic gradient in the HKE treatment. However, the HKE treatment had a lower infiltration rate compared with the LKE treatment during the crusting period. We can conclude from this evidence that the infiltration rate was mainly controlled by the crusting process. This conclusion is consistent with previous studies (Agassi et al., 1981; Leguédois and Le Bissonnais, 2004; Wakindiki and Ben-Hur, 2002).

Crusts formed faster on the HKE treatment compared with the LKE treatment because of the higher energy of raindrops. Although the crusts developed at different speeds, the infiltration rates were similar for both treatments at the end of the rainfall. Smith et al. (1990) also found no difference in the final infiltration rate between medium kinetic energy (KE) rain (8 J m^{-1} mm^{-2}) and high-KE rain (12.4 J m^{-1} mm^{-2}), but they found a significantly lower final infiltration rate for the low-KE rain (3.6 J m^{-1} mm^{-2}). This occurred because the surface crust fully developed under the medium- and high-KE rain but did not form under the low-KE rain. In this study, crusts fully formed in both the HKE and LKE treatments, and similar microstructures were observed for the structural and sedimentary crusts, respectively. These crusts reduced the infiltration rate to the same extent, explaining the similar final infiltration rate of the HKE and LKE treatments. Because the microtopography did not allow for significant puddle development, changes in the water runoff rate showed an inverse trend compared to the infiltration rate, which is not discussed here. Because a high infiltration rate persisted longer for the LKE treatment than for the HKE treatment, percolation was observed only in the LKE treatment. After 45 mm of rainfall, percolation in the LKE treatment started to decrease because of crusting development.

Soil erosion at the outlet was controlled by soil detachment and overland flow (Wakindiki and Ben-Hur, 2002), both of which were affected by the formation of crusts. For the HKE treatment, at first, the soil erosion increased with cumulative rainfall because of the combined increases of disaggregation of surface aggregates, the splash rate, and water runoff. After the crusts fully developed, the erosion rate remained high but started to decrease slightly (Fig. 10). This result is most likely linked to the decrease in the splash rate (Fig. 9). For diffuse erosion, soil detachment is mainly caused by raindrop impacts. Fewer splashed fragments were available to flow transport. For the LKE treatment, the erosion rate increased during the entire rain because both the water runoff and the splash rate increased. A detachment-limited condition was not reached.

Crusting, Erosion, and Agricultural Management

The present results show that (i) Ultisols are prone to crusting, and (ii) the crusts developed on Ultisols significantly decrease water infiltration and promote overland flow and erosion. The kinetic energy of raindrops is a major driver of crust formation. Reducing the kinetic energy of raindrops can significantly slow down crust formation. Therefore, avoiding the soil from being bare would limit crust development. By intercepting raindrop impacts, a vegetation cover, crop residues, or mulch application would likely be beneficial to maintain water infiltration and to limit overland flow and erosion, as shown on other soils in previous studies (Fox et al., 2004; Dalla Rosa et al., 2012).

Roughness, which will depend on cultivation practices, will likely affect crusting and the water and erosion dynamics of Ultisols (Darboux, 2011). However, it is unlikely to alter the above conclusions and recommendations. Detailing its effects could be the purpose of a future study.

Conclusions

Micromorphological observation revealed two types of crusts in this study: structural crust on the ridges and sedimentary crust in the furrows. Structural crusts, mostly 0.3–0.8 mm in thickness, were formed in four stages: (i) initial wetting, (ii) aggregate breakdown by raindrop impact, (iii) fragments transport by splash and overland flow and rearrangement, and (iv) compaction by raindrop impact. Sedimentary crusts, typically > 1 mm in thickness, resulted from the sedimentation of aggregate breakdown products, part of which came from the local area while others were washed down from ridges.

Rainfall kinetic energy played an important role in crust formation. Compared with the HKE rainfall, the LKE rainfall reduced the direct physical impact of raindrops that disintegrated soil aggregates and compacted the soil surface; therefore, the LKE rainfall preserved the soil infiltration capability and delayed the formation of crust. In the LKE treatment, this process resulted in a higher infiltration rate, cumulative infiltration, and percolation but lower splash, runoff, and soil erosion, although the final infiltration rates were similar for the HKE and LKE treatments. This study addressed the importance of rainfall kinetic energy on soil crusting in Ultisols. Keeping the soil surface covered should be an effective way to conserve more water, reduce erosion, and alleviate crusting.

Acknowledgments

The authors appreciate the skilled technical assistance of Lionel Cottenot for the rainfall simulation experiment and Christian Le Lay for making the soil thin sections. This work was supported by (i) the National Key Technology R&D Program of China (2011BAD31B04), (ii) the National Natural Science Foundation of China (grant number 41101200 and 41171180), and (iii) the French National Institute for Agricultural Research (Inra), Department Environment and Agronomy, "Soils" Research Unit.

References

Agassi, M., I. Shainberg, and J. Morin. 1981. Effect of electrolyte concentration and soil sodicity on infiltration rate and crust formation. Soil Sci. Soc. Am. J. 45:848–851. doi:10.2136/sssaj1981.03615995004500050004x

Arshad, M.A., and A.R. Mermut. 1988. Micromorphological and physico-chemical characteristics of soil crust types in northwestern Alberta, Canada. Soil Sci. Soc. Am. J. 52:724–729. doi:10.2136/sssaj1988.03615995005200030024x

Awadhwal, N.K., and G.E. Thierstein. 1985. Soil crust and its impact on crop establishment: A review. Soil Tillage Res. 5:289–302. doi:10.1016/0167-1987(85)90021-2

Betzalel, I., J. Morin, Y. Benyamini, M. Agassi, and I. Shainberg. 1995. Water drop energy and soil seal properties. Soil Sci. 159:13–22. doi:10.1097/00010694-199501000-00002

Dalla Rosa, J., M. Cooper, F. Darboux, and J.C. Medeiros. 2012. Soil roughness evolution in different tillage systems under simulated rainfall using a semivariogram-based index. Soil Tillage Res. 124:226–232. doi:10.1016/j.still.2012.06.001

Darboux, F. 2011. Surface roughness, effect on water transfer. In: J. Glinski, J. Horabik, and J. Lipiec, editors, Encyclopedia of agrophysics. Springer, New York.

Foster, G.R., F.P. Eppert, and L.D. Meyer. 1979. A programmable rainfall simulator for field plots. Proceedings of rainfall simulator workshop, March 7–9, 1979, Tucson, AZ. Agricultural reviews and manuals, ARM-W-10, USDA SEA. pp. 45–59.

Fox, D.M., R.B. Bryan, and A.G. Price. 2004. The role of soil surface crusting in desertification and strategies to reduce crusting. Environ. Monit. Assess. 99:149–159. doi:10.1007/s10661-004-4015-5

Fox, D.M., Y. Le Bissonnais, and P. Quétin. 1998. The implications of spatial variability in surface seal hydraulic resistance for infiltration in a mound and depression microtopography. Catena 32:101–114. doi:10.1016/S0341-8162(98)00043-5

Hu, X., Q. Cai, L. Liu, C. Cai, S. Li, and Y. Zhu. 2005. Development of soil crust through simulated rainfall in laboratory. (in Chinese with English abstract). Acta Ped. Sin. 42:504–507.

Le Bissonnais, Y. 1990. Experimental study and modelling of soil surface crusting processes. In: R.B Bryan, editor, Soil erosion experiments and models. Catena Suppl. 17:13–28.

Le Bissonnais, Y. 1996. Aggregate stability and assessment of soil crustability and erodibility: I. Theory and methodology. Eur. J. Soil Sci. 47:425–437. doi:10.1111/j.1365-2389.1996.tb01843.x

Le Bissonnais, Y., A. Bruand, and M. Jamagne. 1989. Laboratory experimental study of soil crusting: Relation between aggregate breakdown mechanisms and crust structure. Catena 16:377–392. doi:10.1016/0341-8162(89)90022-2

Le Bissonnais, Y., and M.J. Singer. 1992. Crusting, runoff, and erosion response to soil water content and successive rainfalls. Soil Sci. Soc. Am. J. 56:1898–1903. doi:10.2136/sssaj1992.03615995005600060042x

Lee, S.S., C.J. Gantzer, A.L. Thompson, S.H. Anderson, and R.A. Ketcham. 2008. Using high-resolution computed tomography analysis to characterize soil-surface seals. Soil Sci. Soc. Am. J. 72:1478–1485. doi:10.2136/sssaj2007.0421

Legout, C., S. Leguédois, and Y. Le Bissonnais. 2005. Aggregate breakdown dynamics under rainfall compared with aggregate stability measurements. Eur. J. Soil Sci. 56:225–238. doi:10.1111/j.1365-2389.2004.00663.x

Leguédois, S., and Y. Le Bissonnais. 2004. Size fractions resulting from an aggregate stability test, interrill detachment and transport. Earth Surf. Process. Landf. 29:1117–1129. doi:10.1002/esp.1106

Levin, J., M. Ben-Hur, M. Gal, and G. Levy. 1991. Rain energy and soil amendments effects on infiltration and erosion of three different soil types. Aust. J. Soil Res. 29:455–465. doi:10.1071/SR9910455

Li, Z., T. Wang, Z. Shi, S. Ding, and C. Cai. 2005. Relationship between top soil structure changes and erosion process of red soil under simulated rainfall. (in Chinese with English abstract). J. Soil Water Conserv. 19:1–9.

Liang, Y., B. Zhang, X.Z. Pan, and D.M. Shi. 2008. Current status and comprehensive control strategies of soil erosion for hilly region in the Southern China. (in Chinese with English abstract.) Sci. Soil Water Conserv. 6(1):22–27.

McIntyre, D. 1958a. Permeability measurements of soil crusts formed by raindrop impact. Soil Sci. 85:185–189. doi:10.1097/00010694-195804000-00002

Mcintyre, D.S. 1958b. Soil splash and the formation of surface crusts by raindrop impact. Soil Sci. 85:261–266. doi:10.1097/00010694-195805000-00005

Miralles-Mellado, I., Y. Cantón, and A. Solé-Benet. 2011. Two-dimensional porosity of crusted silty soils: Indicators of soil quality in semiarid rangelands? Soil Sci. Soc. Am. J. 75:1330–1342. doi:10.2136/sssaj2010.0283

Moore, D.C., and M.J. Singer. 1990. Crust formation effects on soil erosion processes. Soil Sci. Soc. Am. J. 54:1117–1123. doi:10.2136/sssaj1990.03615995005400040033x

Morin, J., Y. Benyamini, and A. Michaeli. 1981. The effect of raindrop impact on the dynamics of soil surface crusting and water movement in the profile. J. Hydrol. 52:321–335. doi:10.1016/0022-1694(81)90178-5

Morin, J., and J. Van Winkel. 1996. The effect of raindrop impact and sheet erosion on infiltration rate and crust formation. Soil Sci. Soc. Am. J. 60:1223–1227. doi:10.2136/sssaj1996.03615995006000040038x

Murphy, C.P. 1986. Thin section preparation of soils and sediments. A.B. Academic Publishers, Berkhamsted, UK.

Norton, L.D. 1987. Micromorphological study of surface seals developed under simulated rainfall. Geoderma 40:127–140. doi:10.1016/0016-7061(87)90018-8

Reichert, J.M., L.D. Norton, and C. Huang. 1994. Sealing, amendment, and rain intensity effects on erosion of high-clay soils. Soil Sci. Soc. Am. J. 58:1199–1205. doi:10.2136/sssaj1994.03615995005800040028x

Shainberg, I., and M.J. Singer. 1988. Drop impact energy-soil exchangeable sodium percentage interactions in seal formation. Soil Sci. Soc. Am. J. 52:1449–1452. doi:10.2136/sssaj1988.03615995005200050046x

Shi, Z., F. Yan, L. Li, Z. Li, and C. Cai. 2010. Interrill erosion from disturbed and undisturbed samples in relation to topsoil aggregate stability in red soils from subtropical China. Catena 81:240–248. doi:10.1016/j.catena.2010.04.007

Slattery, M.C., and R.B. Bryan. 1994. Surface seal development under simulated rainfall on an actively eroding surface. Catena 22:17–34. doi:10.1016/0341-8162(94)90063-9

Smith, H., G. Levy, and I. Shainberg. 1990. Water-droplet energy and soil amendments: Effect on infiltration and erosion. Soil Sci. Soc. Am. J. 54:1084–1087. doi:10.2136/sssaj1990.03615995005400040026x

Stoops, G. 2003. Guidelines for the analysis and description of soil and regolith thin sections. SSSA, Madison, WI.

Wakindiki, I.I.C., and M. Ben-Hur. 2002. Soil mineralogy and texture effects on crust micromorphology, infiltration, and erosion. Soil Sci. Soc. Am. J. 66:897–905. doi:10.2136/sssaj2002.0897

Yang, W., Z. Li, C. Cai, J. Wang, and Z. Hua. 2012. Tensile strength and friability of Ultisols in sub-tropical China and effects on aggregate breakdown under simulated rainfall. Soil Sci. 177:377–384. doi:10.1097/SS.0b013e31824d913e